

Curcumin induces ferroptosis and apoptosis in osteosarcoma cells by regulating Nrf2/GPX4 signaling pathway

Chuanjian Yuan^{1*}, Rong Fan^{2*}, Kai Zhu^{1,3}, Yutong Wang¹, Wenpeng Xie⁴ and Yanchen Liang⁴ 

¹First Clinical College, Shandong University of Traditional Chinese Medicine, Jinan 250014, China; ²Yantai Raphael Biotechnology Co., Ltd, Yantai 264000, China; ³Department of Orthopedics, Gaoqing Traditional Chinese Medicine Hospital Co., Ltd, Zibo 256300, China; ⁴Department of Orthopedics, Affiliated Hospital of Shandong University of Traditional Chinese Medicine, Jinan 250014, China

*These authors contributed equally to this paper.

Corresponding authors: Yanchen Liang. Email: 71000360@sducm.edu.cn; Wenpeng Xie. Email: xiewenpeng0925@163.com

Impact Statement

Curcumin was an antitumor agent to inhibit cell growth and metastasis in osteosarcoma. This study aimed to investigate the effects and potential mechanisms of curcumin on osteosarcoma both *in vitro* and *in vivo*. It can provide some evidence for curcumin to become a potential therapy drug for osteosarcoma in the future.

Abstract

Curcumin, an antitumor agent, has been shown to inhibit cell growth and metastasis in osteosarcoma. However, there is no evidence of curcumin and its regulation of cell ferroptosis and nuclear factor E2-related factor 2 (Nrf2)/glutathione peroxidase 4 (GPX4) signaling pathways in osteosarcoma. This study aimed to investigate the effects of curcumin on osteosarcoma both *in vitro* and *in vivo*. To explore the effects and mechanisms of curcumin on osteosarcoma, cells (MNNG/HOS and MG-63) and xenograft mice models were established. Cell viability, cell apoptosis rate, cycle distribution, cell migration, cell invasion, reactive oxygen species, malonaldehyde and glutathione abilities, and protein levels were detected by cell counting kit-8, flow cytometry, wound healing, transwell assay, respectively. Nrf2 and GPX4 expressions

were detected using an immunofluorescence assay. Nrf2/GPX4-related protein levels were detected using western blotting. The results showed that curcumin effectively decreased cell viability and increased apoptosis rate. Meanwhile, curcumin inhibited tumor volume in the xenograft model, and Nrf2/GPX4-related protein levels were also altered. Interestingly, the effects of curcumin were reversed by liproxstatin-1 (an effective inhibitor of ferroptosis) and bardoxolone-methyl (an effective activator of Nrf2). Our results indicate that curcumin has therapeutic effects on osteosarcoma cells and a xenograft model by regulating the expression of the Nrf2/GPX4 signaling pathway.

Keywords: Osteosarcoma, ferroptosis, Nrf2/GPX4, ROS, GSH

Experimental Biology and Medicine 2024; 248: 2183–2197. DOI: 10.1177/15353702231220670

Introduction

Osteosarcoma, accounting for 60% of primary bone tumors, is a major form of primary bone malignancy in young adults and children.^{1–3} Even after aggressive surgical strategies, chemotherapy, and radiotherapy, patients with osteosarcoma still have highly malignant and metastatic conditions with a poor prognosis.⁴ Therefore, it is important to prevent the progression of osteosarcoma and develop targeted therapeutic strategies.

Osteosarcomas mostly develop from mesenchymal stem cells (MSCs). As cells inside the bone begin to divide uncontrollably, osteosarcoma occurs and can be extremely aggressive and has distal metastatic properties.^{5,6} Apoptosis, autophagy, necrosis, and pyroptosis are regular forms of cell death.⁷ Ferroptosis, a new form of cell death, is mediated

by intracellular iron and is clearly distinguished from other forms of cell death forms.^{8,9} Recently, emerging evidence has highlighted that aberrant cellular iron metabolism can induce overproduction of reactive oxygen species (ROS) and trigger lipid peroxidation (LPO). However, aberrant generation of ROS and LPO would cause DNA and RNA damage, thereby inducing the hallmarks of ferroptosis and non-apoptotic programmed cell death.^{10,11} The hallmarks of ferroptosis including dysmorphic mitochondria, decreased mitochondrial cristae, and diminished mitochondrial membrane.¹²

In addition, various studies have found that ferroptosis can be regulated by glutathione peroxidase 4 (GPX4), the mevalonate pathway, lipid synthesis, the transcription factor nuclear factor E2-related factor 2 (Nrf2/NFE2L2) pathway and other factors.^{13,14} GPX4 is an enzyme that removes lipid peroxide. In addition, Nrf2 can regulate GPX4 and free

iron content, thereby regulating ferroptosis. Studies have revealed that some clinical drugs induce ferroptosis in cancers, thereby inhibiting the progression of cancer.¹⁵

Curcumin, a natural phenolic compound extracted from *Curcuma longa* exhibits various pharmacological activities, including antitumor, antioxidant, and anti-inflammatory activities, via modulation of intracellular signaling pathways.^{16,17} Studies have shown that the anticancer effects of curcumin have been found in various cancer types, including breast, prostate, colon, and osteosarcoma.^{18–20} Curcumin has been shown to exert antitumor activities by regulating intracellular signaling pathways, such as RANK/RANKL, Notch, Wnt/ β -catenin, and ferroptosis, relative to the SLC7A11, GPX4, HO-1, and HMOX1 pathways.²¹

Curcumin, as an antitumor agent, has been shown to inhibit cell growth and metastasis in osteosarcoma.^{22,23} Many studies have reported that curcumin can inhibit the production of ROS, metastasis, angiogenesis, and osteoclast formation, thereby suppressing osteosarcoma development.²⁴ However, there are few studies on the ability of curcumin to regulate ferroptosis in osteosarcoma.²⁵

Based on the aforementioned literature, in the recent research, we aimed to explore the effects of curcumin on osteosarcoma cells and mice model. In addition, we explored the effects of curcumin and its regulation of cell ferroptosis and Nrf2/GPX4 signaling pathways. This study aimed to provide a scientific reference for research on the mechanism of curcumin and identify a novel therapeutic target of curcumin for osteosarcoma.

Materials and methods

Cell culture and groups

Human osteosarcoma cell lines MNNG/HOS and MG-63 were purchased from KeyGEN BioTECH (Jiangsu, China). The cells were incubated in Eagle's Minimum Essential Medium, supplemented with 10% fetal bovine serum (FBS) and 1% penicillin/streptomycin, cultured in a humid incubator at 37°C with 5% CO₂.

Cells were divided into five groups: control group; curcumin group (cells treated with 22.5 μ M curcumin); erastin group (cells treated with 20 μ M erastin); curcumin + liproxstatin-1 (Lip-1) group (cells treated with 22.5 μ M curcumin and 80 nM Lip-1); curcumin + bardoxolone-methyl (BM) group (cells treated with 22.5 μ M curcumin and 0.05 μ M BM).²⁶

Cell viability assay

Cell counting kit-8 (CCK-8) kit (KeyGEN BioTECH) was used to detect MNNG/HOS and MG-63 cell viability. Briefly, MNNG/HOS and MG-63 cells were seeded into 96-well plates at a density of 3.0×10^3 /well and cultured for 24 h. Cells were incubated with CCK-8 solution (10 μ L) at 24, 48, and 72 h, and cultured in an incubator at 37°C for 2 h, and measured using a microplate detector (BD Biosciences, San Jose, CA, USA) at 450 nm optical density.

Transwell assay

A transwell assay was performed to detect MNNG/HOS and MG-63 cell invasion rates. Chamber with an 8-mm pore membrane was used according to the manufacturer's instructions and previous studies.²⁷ Briefly, cells were collected and counted after treatment with curcumin or other drugs. A total of 1×10^4 cell suspension was added to each upper chamber (the inner bottom was pre-coated with Matrigel Matrix). Next, 500 μ L of growth medium containing 10% serum was added to the lower chamber. Then, the cells were incubated at 37°C in a 5% CO₂ for 48 h. Cells were stained with 0.5% crystal violet, and the invasiveness of cells on the lower side was examined using an inverted microscope.

Cell apoptosis assay

MNNG/HOS and MG-63 cell apoptosis in different experimental groups was measured using an Annexin V-fluorescein isothiocyanate (FITC)/propidium iodide (PI) apoptosis detection kit (BD Biosciences), according to the manufacturer's instructions.²⁸ MNNG/HOS and MG-63 cells in the logarithmic growth phase were collected and inoculated into a six-well plate. Then, 5 μ L of Annexin V-FITC and PI was added to the sample for 15 min in the dark and detected by flow cytometry (BD Biosciences).

ROS detection assay

To quantify the levels of ROS, the dichlorodihydrofluorescein diacetate (DCFH-DA) probe was employed following the guidelines provided by the manufacturer. In brief, cells were seeded in six-well plates and treated with quercetin. Subsequently, the cells were harvested, rinsed twice with phosphate-buffered saline (PBS), and subjected to labeling with 20 mM DCFH-DA in a light-restricted environment for a duration of 30 min. The fluorescence intensity of the collected cells was determined using a flow cytometer. All experimental steps were conducted in accordance with the manufacturer's instructions.²⁹

Cell cycle distribution

MNNG/HOS and MG-63 cell cycle distributions were detected using a cell cycle detection kit (KeyGEN BioTECH). All procedures were performed in accordance with the manufacturer's instructions.³⁰ Briefly, cells were collected after different treatment measures. Cells were resuspended in ethanol (75%) overnight. PI/RNase mix (500 μ L) was added and flow cytometry (BD Biosciences) was used to detect the cell cycle distribution.

Transmission electron microscopy assay. Transmission electron microscopy (TEM) assays were performed in accordance with established protocols. After trypsinization, MNNG/HOS and MG-63 cells were centrifuged at 225g for 5 min and subsequently fixed with 4% glutaraldehyde for 2 h at 4°C. Sections were stained with uranyl acetate and lead citrate. TEM images were captured using a JEM-1400Plus transmission electron microscope.

Immunohistochemical analysis

The expression of Nrf2 and GPX4 was detected by immunofluorescence with a Deacetylase Fluorometric Assay kit (Bio Vision, Inc., Milpitas, CA, USA) according to the manufacturer's instructions. Fluorescence microscopy was used to observe Nrf2 and GPX4 positive cells, and the images were photographed.

Establishment of xenograft model

Fifty BALB/c nude mice were used to establish a xenograft model. MNNG/HOS cells were injected into the left axilla of the nude mice at a dose of 1×10^7 . After tumor formation, the mice were divided into five groups ($n=10$): control, curcumin, erastin, curcumin + lip-1, and curcumin + baradoxolone-methyl. The tumors were measured using an electronic Vernier caliper, and the tumor volume and growth rate were calculated. We followed the ARRIVE guidelines point-by-point during experimental studies (Animal Research: Reporting of In Vivo Experiments), and all animal procedures were approved by the Shandong University of Traditional Chinese Medicine. All animal maintenance and operational procedures were performed in accordance with the Guide for the Care and Use of Laboratory Animals published by the National Institutes of Health (NIH Publication no. 86-23, revised 1996).

Measurement of malondialdehyde and glutathione

Malondialdehyde (MDA) and glutathione (GSH) assay kits were used to measure the MDA and GSH concentrations. The experiment was performed according to the manufacturer's instructions.

Immunohistochemical staining assay

According to previous studies, immunohistochemical staining assay was performed.³¹ An immunohistochemical kit (Millipore; Merck KGaA, Darmstadt, Germany) was used to assess Nrf2 expression. Optical microscopy (Olympus Corp., Tokyo, Japan) was used to observe apoptotic cells, and images were photographed at $200\times$ magnification.

Western blotting

The experimental procedure was performed as previously described in the previous study.³² The total protein concentrations of the cells and tissues were measured using the BCA protein quantification method (Beyotime, China). Equal amounts of protein were resolved by electrophoresis on a 10% sodium dodecyl-sulfate (SDS) gel and then transferred onto nitrocellulose membranes. Following blocking by incubation in 5% non-fat milk, membranes were probed with specific anti-SLC7A11 (Cell Signaling Technology, 1:1000), anti-GPX4 (Cell Signaling Technology, 1:1000), anti-HO-1 (Cell Signaling Technology, 1:1000), anti-Nrf2 (Abcam, 1:1500), and β -actin (Abcam, 1:1000) overnight at 4°C . After washing with tris-buffered saline (TBS) containing 0.24% Tween-20, the membranes were incubated for 60 min with horseradish peroxidase-conjugated secondary antibody. An enhanced chemiluminescence system was used for

visualization of protein signals, and the density of each protein band was analyzed using Image-Pro Plus6.0 (Media Cybernetics, Silver Spring, MD, USA).

Statistical analysis

All experimental data were analyzed using IBM SPSS Statistics (version 19.0, SPSS, Inc., Chicago, IL, USA). The significant difference of data for comparison was analyzed by one-way analysis of variance (ANOVA) followed by Tukey's post-test. The data were considered significantly different at $P < 0.05$.

Results

Effects of curcumin on cell viability, cell apoptosis rate, and cell cycle in MNNG/HOS and MG-63 cells

To investigate the effects of curcumin on cell viability, apoptosis rate, and cell cycle, CCK-8 and flow cytometry assays were performed. As shown in Figure 1(A) and (B), our results revealed that after treatment with curcumin ($22.5\ \mu\text{M}$), cell viability was significantly decreased ($P < 0.05$ versus control group), while the cell viability in the erastin group was similarly decreased. However, compared to the curcumin group, after treatment with Lip-1 or BM, cell viability was significantly increased ($P < 0.05$).

Consistent with the CCK-8 assay results, the cell apoptosis rate results (Figure 1(C) and (D)) revealed that after treatment with curcumin, the cell apoptosis rate was significantly increased ($P < 0.05$ versus control group), while the cell apoptosis rate in the erastin group was similarly increased. However, compared to the curcumin group, after treatment with Lip-1 or BM, the cell apoptosis rate was significantly lower ($P < 0.05$).

As shown in Figure 2(A) and (B), cell cycle distribution results revealed that after treatment with curcumin, the percentage of cells undergoing sub G0/G1 phase in both cell lines gradually increased. These results indicate that curcumin induced G0/G1 phase arrest.

Curcumin reversed cell invasion in MNNG/HOS and MG-63 cells

To further investigate the effects of curcumin on migration and cell invasion, wound healing and transwell assays were performed. As shown in Figure 3(A) and (B), our results revealed that after treatment with curcumin, cell invasion abilities were significantly decreased ($P < 0.05$ versus control group), while cell invasion abilities in the erastin group were similarly decreased. However, compared with the curcumin group, after treatment with Lip-1 or BM, cell invasion abilities were significantly increased ($P < 0.05$).

Curcumin reversed ROS levels in MNNG/HOS and MG-63 cells

Growing evidence has revealed that the lipid and amino acid metabolic pathways are involved in the regulation of ferroptosis. Ferroptosis is characterized by the accumulation of lipid hydroperoxides and ROS derived from iron metabolism. It can be triggered in cancer cells by depleting

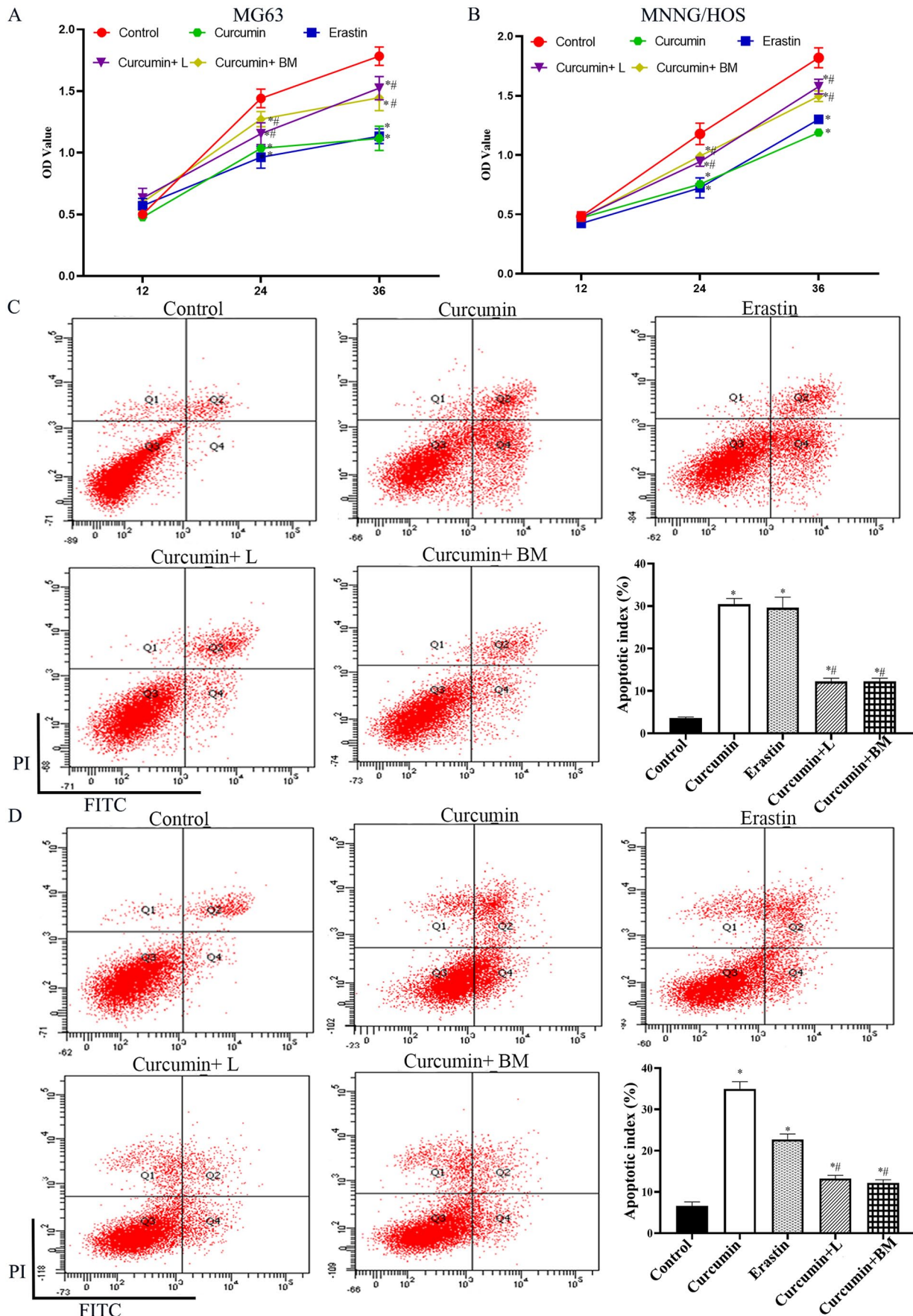


Figure 1. Effects of curcumin on cell viability and cell apoptosis rate in MG-63 and MNNG/HOS cells ($n=6$): (A) MG-63 cell viability was detected by CCK-8 assay, (B) MNNG/HOS cell viability was detected by CCK-8 assay, (C) MG-63 cell apoptosis rate was detected by flow cytometry, and (D) MNNG/HOS cell apoptosis rate. * $P < 0.05$ versus control group; # $P < 0.05$ versus curcumin group.

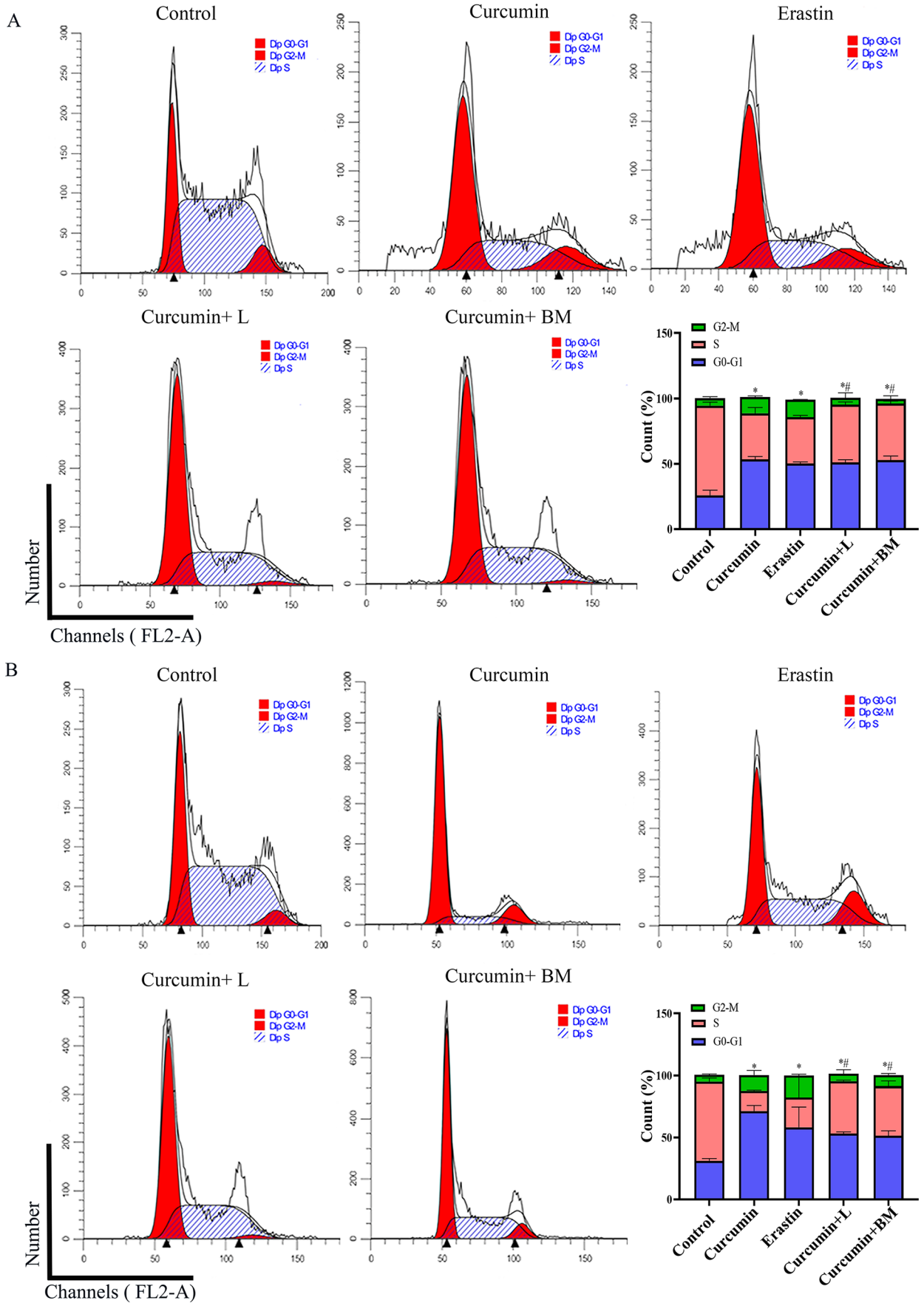


Figure 2. Effects of curcumin on cell cycle distribution in MG-63 and MNNG/HOS cells (n=6): (A) cell cycle distribution in MG-63 cells and (B) cell cycle distribution in MNNG/HOS cells.

*P < 0.05 versus control group; #P < 0.05 versus curcumin group.

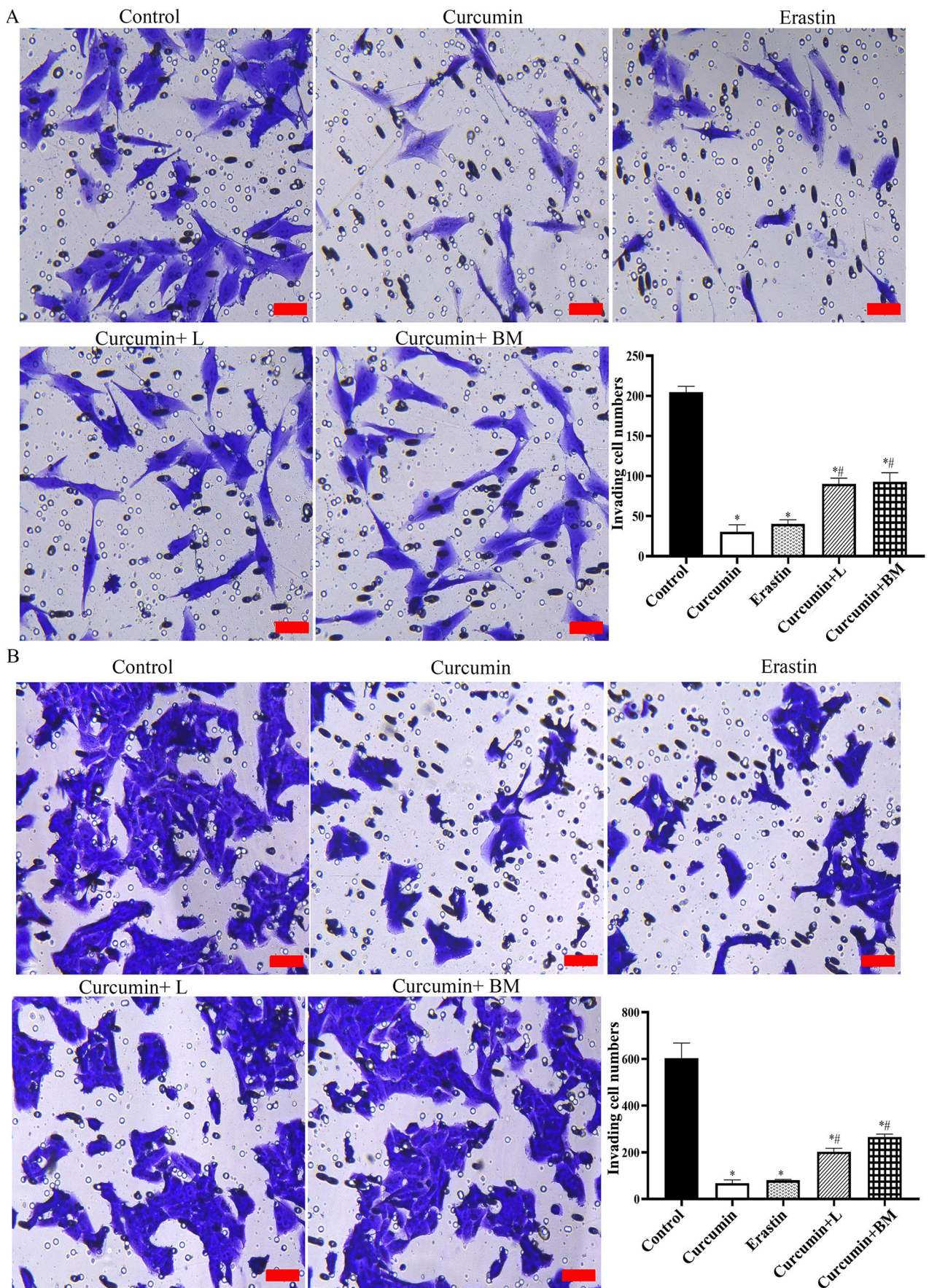


Figure 3. Effects of curcumin on cell invasion in MG-63 and MNGG/HOS cells ($n=6$): (A) MG-63 cell invasion rate was detected by transwell assay (scar bar: 50 μm) and (B) MNGG/HOS cell invasion rate was detected by transwell assay (scar bar: 50 μm).
 $*P < 0.05$ versus control group; $\#P < 0.05$ versus curcumin group.

GSH or inhibiting GPX4. To further investigate the effects of curcumin on ROS levels, flow cytometry was performed. As shown in Figure 4(A) and (B), our results revealed that after treatment with curcumin, ROS levels were significantly increased ($P < 0.05$ versus control group). However, compared with the curcumin group, after treatment with Lip-1 or BM, ROS and GSH levels were significantly changed ($P < 0.05$).

Meanwhile, the immunofluorescence assay results of ROS were found to be consistent with the flow cytometry results, as depicted in Figure 4(C) and (D).

Curcumin induced mitochondrial structural changes in MNNG/HOS and MG-63 cells

In order to improve understanding of the mechanism by which curcumin induces cell death in MNNG/HOS and MG-63 cells, we utilized transmission electron microscopy to analyze the ultrastructural features of cancer cells. Our observations, as illustrated in Figure 5(A) and (B), revealed that in the group treated with curcumin, the cell membrane exhibited fragmentation and vesiculation, the mitochondria displayed reduced size, increased membrane density, diminished or absent mitochondrial ridges, and disrupted outer membrane. The nucleus size remained normal, although chromatin condensation was not observed. Further examination under an electron microscope revealed a reduction in mitochondrial size and an increase in membrane density, which are indicative of ferroptosis, a significant phenomenon.

Curcumin reversed Nrf2 and GPX4 expressions in MNNG/HOS and MG-63 cells

To investigate the effects of curcumin on Nrf2 and GPX4 expressions, immunofluorescence assay was performed. As shown in Figure 6(A) and (B), our results revealed that after treatment with curcumin, Nrf2 and GPX4 levels were significantly decreased. Meanwhile, in erastin group, Nrf2 and GPX4 levels were significantly decreased. However, compared with the curcumin group, after treatment with Lip-1 or BM, Nrf2 and GPX4 levels were significantly increased.

Curcumin reversed Nrf2/GPX4 relative protein levels in MNNG/HOS and MG-63 cells

To investigate the effects of curcumin on Nrf2/GPX4 relative protein levels, western blotting was performed. As shown in Figure 7(A) to (J), our results revealed that after treatment with curcumin, Nrf2, SLC7A11, HO-1, and GPX4 protein levels were decreased ($P < 0.05$ versus control group), while in the erastin group, Nrf2, SLC7A11, HO-1, and GPX4 protein levels were decreased ($P < 0.05$ versus control group). However, compared with the curcumin group, after treatment with Lip-1 or BM, Nrf2, SLC7A11, HO-1, and GPX4 protein levels increased ($P < 0.05$).

Curcumin inhibited the tumor volume and increased cell apoptosis rate in xenograft model

To further evaluate the effects of curcumin on tumor growth, an MNNG/HOS xenograft model was constructed. As shown in Figure 8(A) and (B), compared to the control group,

the tumor growth curve indicated that the tumor volume in the curcumin group was significantly smaller ($P < 0.05$). Meanwhile, the tumor volume in the erastin group was significantly smaller ($P < 0.05$). Accordingly, compared to the curcumin group, after treated with Lip-1 or BM, the tumor volume was significantly bigger ($P < 0.05$).

As shown in Figure 8(C), the cell apoptosis rate results revealed that after treatment with curcumin, the cell apoptosis rate was significantly increased ($P < 0.05$ versus control group), while the cell apoptosis rate in the erastin group was similarly increased. However, compared to the curcumin group, after treatment with Lip-1 or BM, the cell apoptosis rate was significantly lower ($P < 0.05$).

Curcumin reversed ROS, MDA, and GSH levels in xenograft model

To further investigate the effects of curcumin on ROS, MDA and GSH levels, an enzyme-linked immunosorbent assay (ELISA) was performed. As shown in Figure 8(D) to (F), our results revealed that after treatment with curcumin, ROS and MDA levels were significantly increased while GSH levels were decreased ($P < 0.05$ versus control group). However, compared to the curcumin group, after treatment with Lip-1 or BM, ROS, MDA, and GSH levels were significantly changed ($P < 0.05$).

Curcumin reversed Nrf2 and GPX4 expressions in xenograft model

To investigate the effects of curcumin on Nrf2 and GPX4 expressions, immunofluorescence assay was performed. As shown in Figure 9(A), our results revealed that after treatment with curcumin, Nrf2 and GPX4 levels were significantly decreased. Meanwhile, in erastin group, Nrf2 and GPX4 levels were significantly decreased. However, compared with the curcumin group, after treatment with Lip-1 or BM, Nrf2 and GPX4 levels were significantly increased.

Curcumin reversed Nrf2/GPX4 relative protein levels in xenograft model

To further investigate the effects of curcumin on Nrf2/ GPX4 relative protein levels, western blotting was performed. As shown in Figure 9(B) to (F), our results revealed that after treatment with curcumin, Nrf2, SLC7A11, HO-1, and GPX4 protein levels were decreased ($P < 0.05$ versus control group), while in the erastin group, Nrf2, SLC7A11, HO-1, and GPX4 protein levels were decreased ($P < 0.05$ versus control group). However, compared with the curcumin group, after treatment with Lip-1 or BM, Nrf2, SLC7A11, HO-1, and GPX4 protein levels increased ($P < 0.05$).

Discussion

Various studies have indicated that ferroptosis is a new form of programmed cell death induced by LPO, followed by iron release and lethal ROS.^{33,34} In this study, we investigated the effects of curcumin on osteosarcoma. Our results revealed that curcumin inhibited the viability, migration, and invasion of MNNG/HOS and MG-63 cells. Meanwhile, ROS, MDA, and GSH levels and Nrf2/ GPX4 relative protein

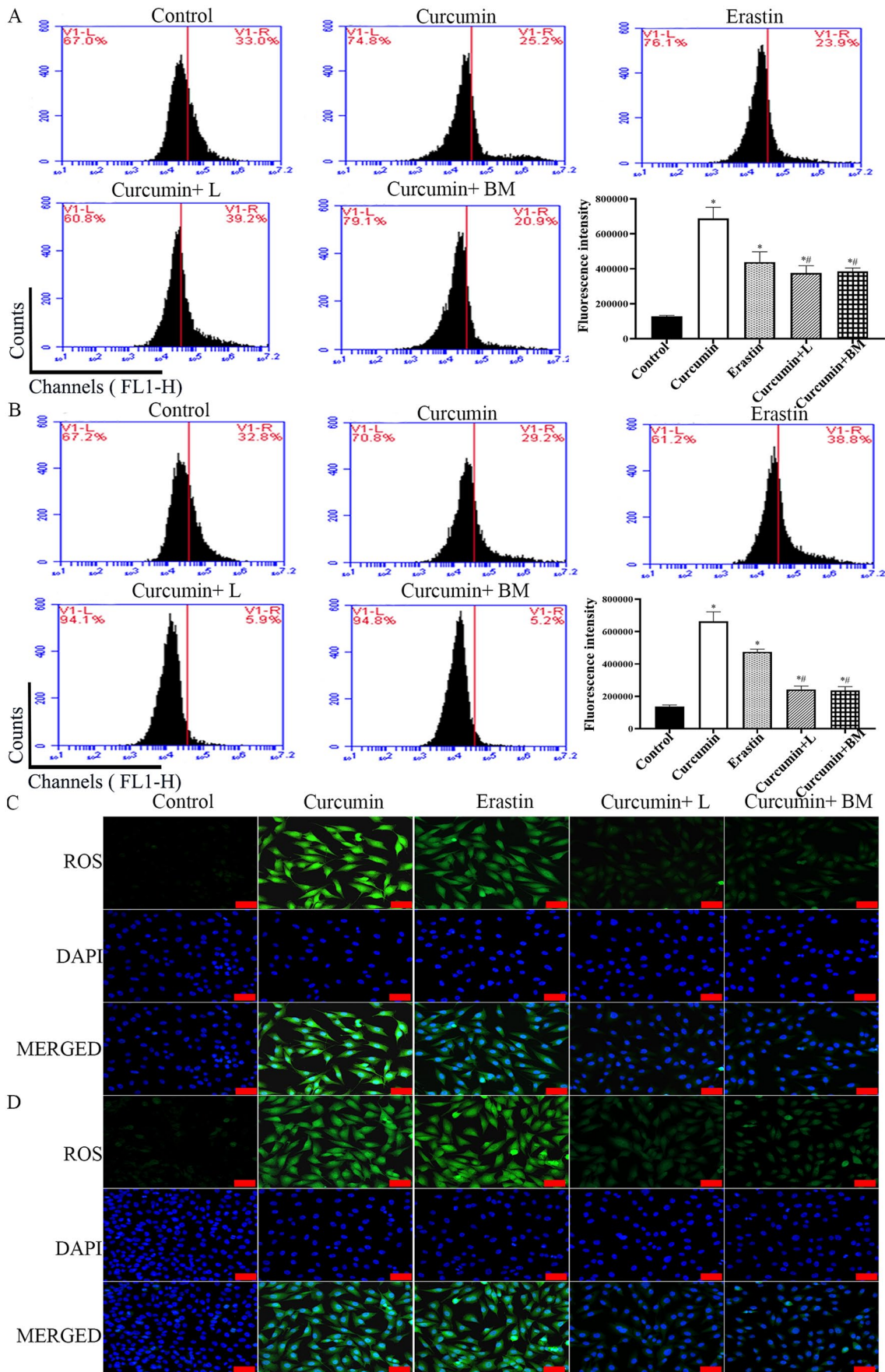


Figure 4. Effects of curcumin on ROS levels in MG-63 and MNNG/HOS cells ($n=6$): (A) ROS levels in MG-63 cells were detected by flow cytometry, (B) ROS levels in MNNG/HOS cells, (C) ROS levels in MG-63 cells were detected by immunofluorescence assay (scar bar: 50 μm), and (D) ROS levels in MNNG/HOS cells were detected by immunofluorescence assay (scar bar: 50 μm).

* $P < 0.05$ versus control group; # $P < 0.05$ versus curcumin group.

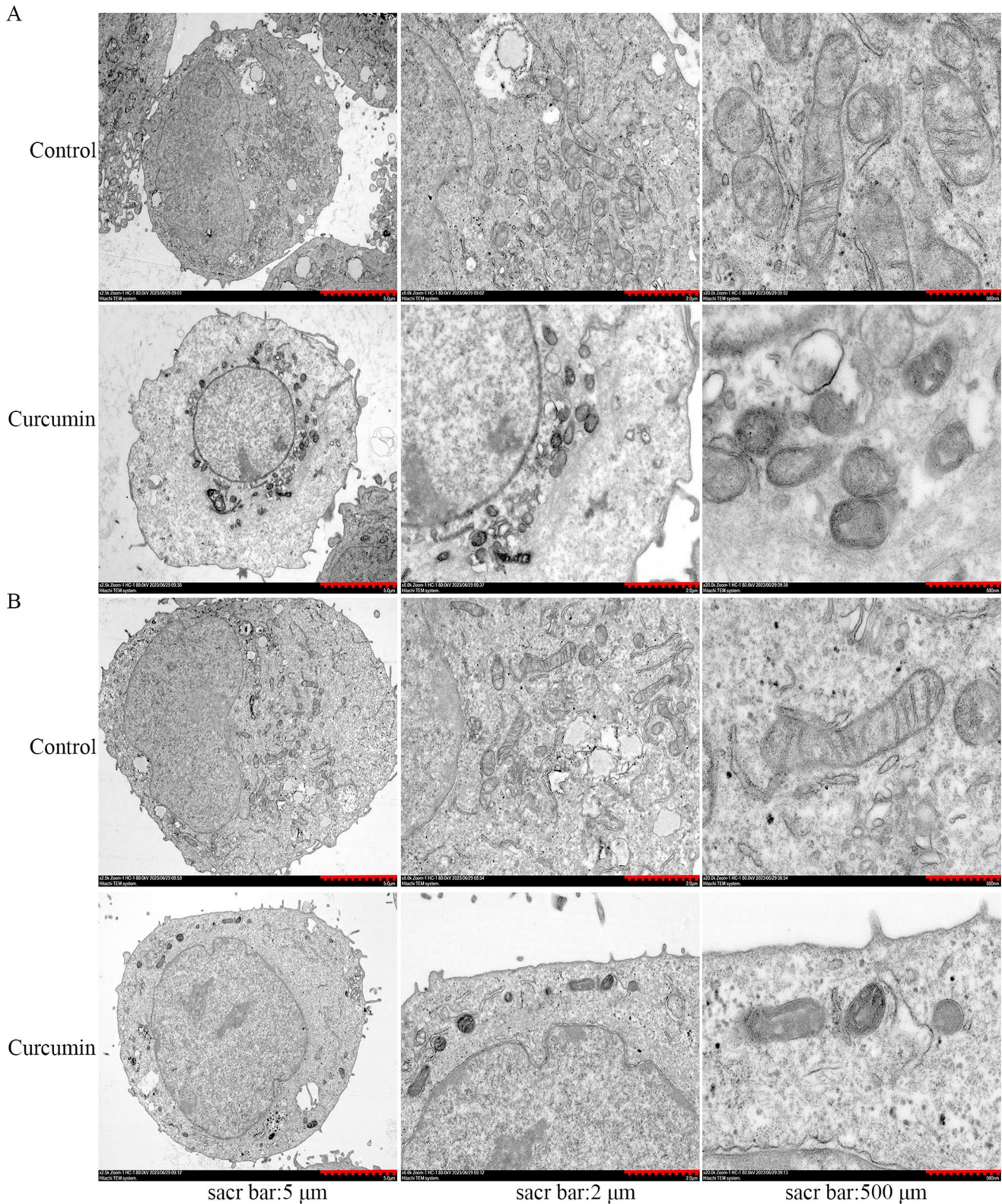


Figure 5. Effects of curcumin on mitochondrial structural changes in MG-63 and MNNG/HOS cells ($n=3$): (A) mitochondrial structural changes in MG-63 cells and (B) mitochondrial structural changes in MNNG/HOS cells.

levels were also changed by treatment with curcumin. Interestingly, there is addition of Lip-1 (an effective inhibitor of ferroptosis) and BM (an effective activator of Nrf2). Taken together, these results revealed that curcumin could induce osteosarcoma cell ferroptosis while mediating progression via the regulation of Nrf2/GPX4 pathway.

The high mortality rate of osteosarcoma is believed to be due to its high rate of metastasis. Invasion and metastasis of osteosarcoma often occur in the early stages.³⁵ With the development of chemotherapy, the survival rate has increased; however, invasion and metastasis remain the main problems for the failure.³⁶ There is an urgent need to

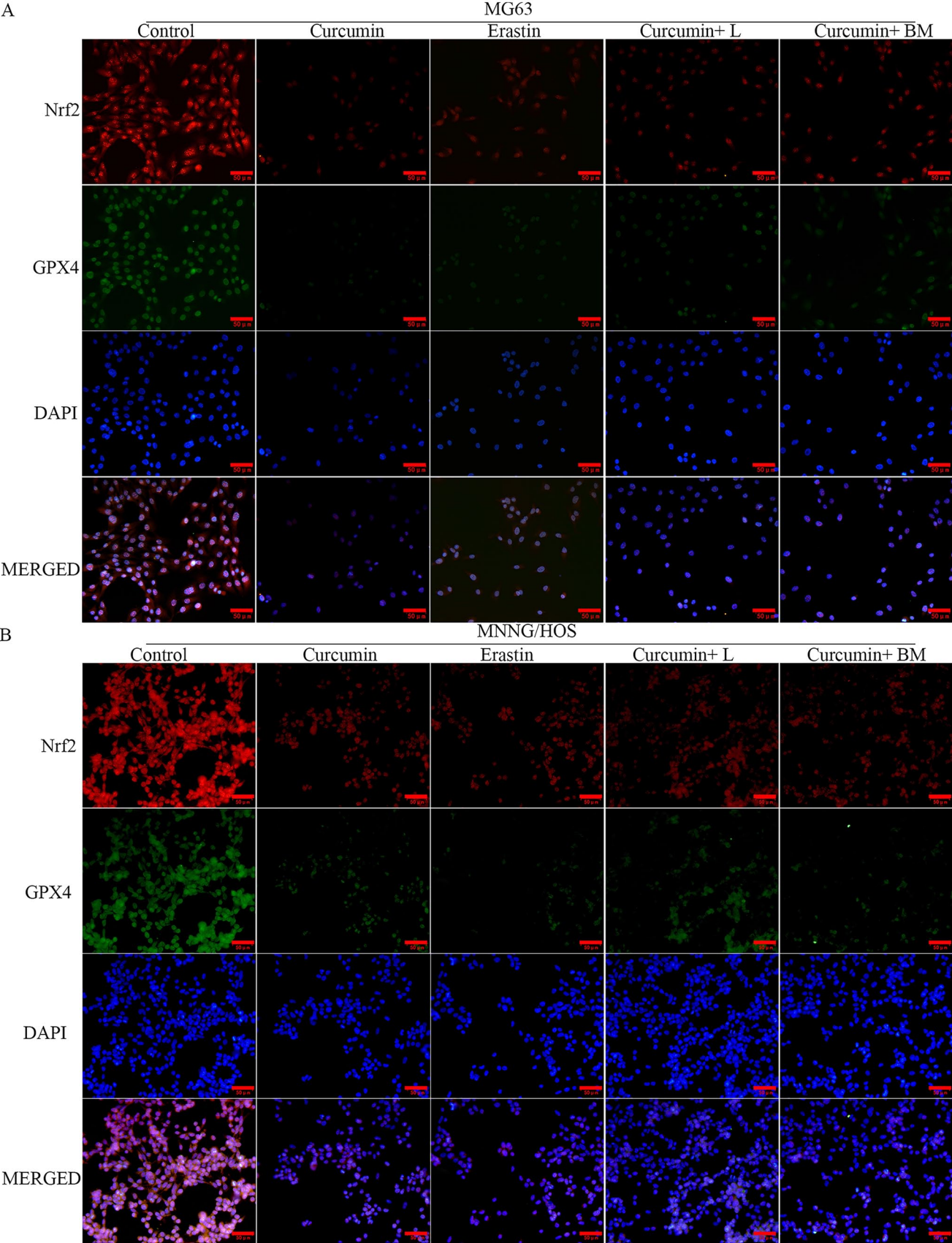


Figure 6. Effects of curcumin on Nrf2 and GPX4 expressions in MG-63 and MNNG/HOS cells (n=6, scar bar: 50 μm): (A) Nrf2 and GPX4 expressions in MG-63 cells and (B) Nrf2 and GPX4 expressions in MNNG/HOS cells.

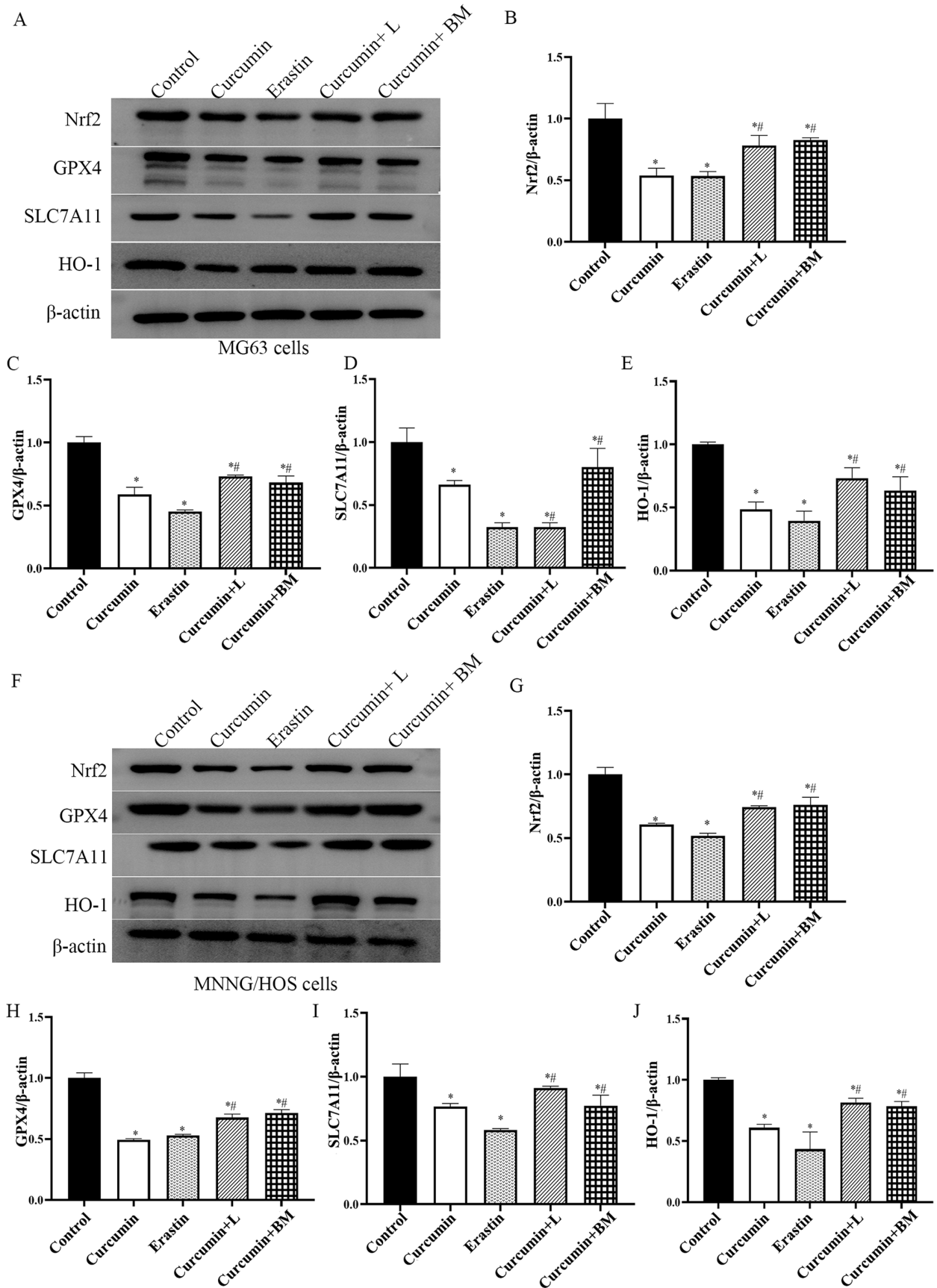


Figure 7. Effects of curcumin on Nrf2/GPX4 related protein levels in MG-63 and MNNG/HOS cells ($n=6$): (A) western blot bands in MG-63 cells, (B) Nrf2 expressions, (C) GPX4 expressions, (D) SLC7A11 expressions, (E) HO-1 expressions, (F) western blot bands in MNNG/HOS cells, (G) Nrf2 expressions, (H) GPX4 expressions, (I) SLC7A11 expressions, and (J) HO-1 expressions.

* $P < 0.05$ versus control group; # $P < 0.05$ versus curcumin group.

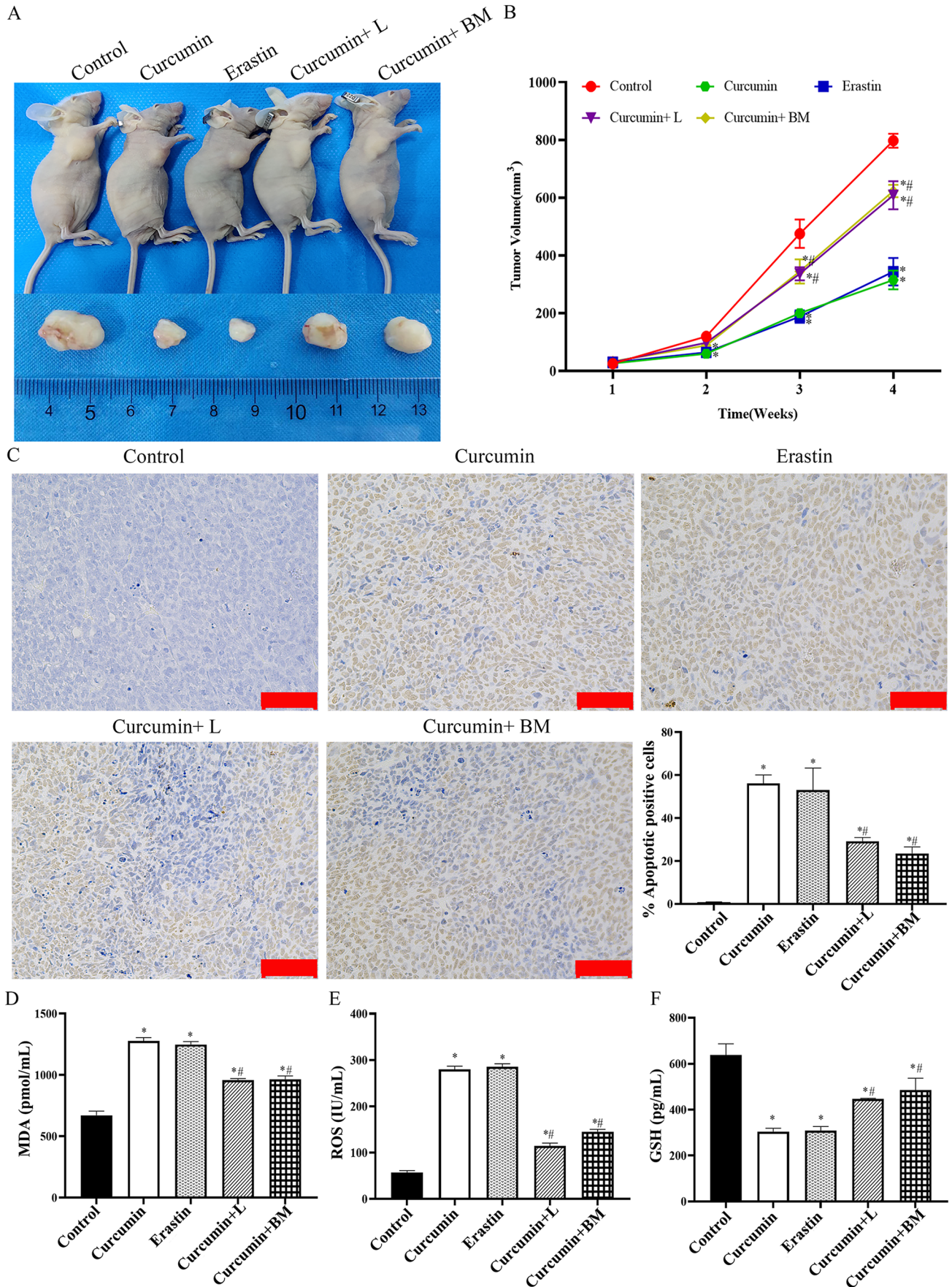


Figure 8. Effects of curcumin on tumor volume, ROS, MDA, and GSH levels in xenograft model ($n=6$): (A) tumor images of MNGG/HOS cells induced xenograft model, (B) tumor volume of xenograft model, (C) cell apoptosis rate was detected by TUNEL assay (scar bar: 50 μ m), (D) MDA levels, (E) ROS levels, and (F) GSH levels. * $P < 0.05$ versus control group; # $P < 0.05$ versus curcumin group.

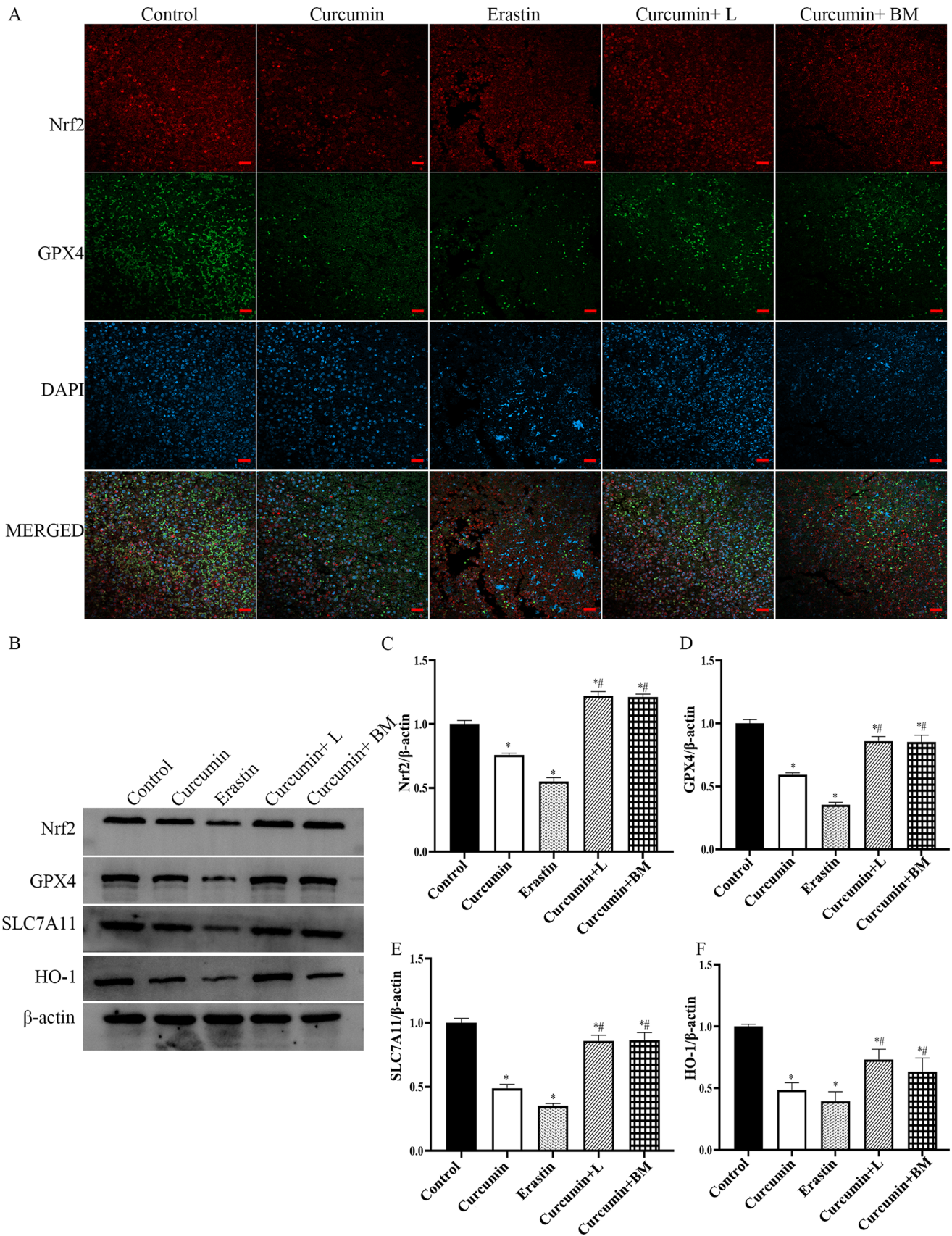


Figure 9. Effects of curcumin on Nrf2, GPX4, and Nrf2/GPX4 relative protein expressions in xenograft model ($n=3$): (A) Nrf2 and GPX4 expressions were detected by immunofluorescence (scar bar: 20 μ m), (B) western blot bands, (C) Nrf2 expressions, (D) GPX4 expressions, (E) SLC7A11 expressions, and (F) HO-1 expressions. * $P < 0.05$ versus control group; # $P < 0.05$ versus curcumin group.

reveal the factors and signaling pathways involved in the metastatic process of human osteosarcoma. Consistent with previous studies, our research revealed that curcumin can inhibit cell viability, migration, and invasion in MNNG/HOS and MG-63 cells. Our results also revealed that curcumin induced G2/M phase arrest, which is consistent with the results of previous studies.

Ferroptosis is a new form of programmed cell death induced by various inducers, such as the accumulation of LPO and ROS.^{37,38} Growing evidence has revealed that the lipid and amino acid metabolic pathways are involved in the regulation of ferroptosis.^{15,39} Ferroptosis is characterized by the accumulation of lipid hydroperoxides and ROS derived from iron metabolism.^{40,41} It can be triggered in cancer cells by depleting GSH or inhibiting GPX4. Growing evidence indicates that Nrf2 is a critical antioxidant transcription factor that mediates ferroptosis. Many components of the ferroptosis cascade are target genes of the transcription factor Nrf2; the downregulating of GPX4, SLC7A11, and ROS activities was related to the progression of ferroptosis.⁴² Studies have revealed that GPX4 is a downstream target of Nrf2, and targeting GPX4 is considered a crucial strategy for triggering ferroptosis. Mechanistically, studies have verified that GSTZ1 knockout could induce cell ferroptosis via activation of the Nrf2/GPX4 axis.^{43,44} In accordance with prior studies, curcumin also exerts an influence on the levels of ROS and MDA. Collectively, these outcomes elucidate the ability of curcumin to induce cell ferroptosis through the modulation of ROS expression and Nrf2/GPX4 protein levels.

Ferroptosis is a new form of programmed cell death induced by various factors, such as LPO and ROS accumulation. Growing evidence indicates that Nrf2 is a critical antioxidant transcription factor that mediates ferroptosis. Many components of the ferroptosis cascade are target genes of the transcription factor Nrf2, and the downregulation of GPX4, SLC7A11, and ROS activities is related to the progression of ferroptosis. Studies have revealed that GPX4 is a downstream target of Nrf2, and targeting GPX4 is considered a crucial strategy for triggering ferroptosis. The activation of the Nrf2/GPX4 axis has been mechanistically confirmed to induce cell ferroptosis. In this particular study, BM, an activator of Nrf2, was employed to investigate the potential mechanisms linking curcumin and Nrf2. Our findings align with previous research, as they reveal that curcumin treatment effectively suppresses the expression of Nrf2, SLC7A11, HO-1, and GPX4 in both *in vivo* and *in vitro* settings.

Nrf2 is a key regulatory factor required by cells to maintain an oxidative steady state. Growing evidence indicates that Nrf2 is a critical antioxidant transcription factor that mediates ferroptosis response.^{20,45} Moreover, studies have revealed that increased Nrf2 expression is associated with poor outcomes and disease-free survival in osteosarcoma. BM is an extremely efficient Nrf2 activator. According to previous studies, BM can induce the release of activated Nrf2, resulting in Nrf2 protein stabilization and nuclear translocation.³⁹ Lip-1 is an effective inhibitor of ferroptosis. BM significantly altered the effects of curcumin. Ferritin is the major intracellular iron storage protein complex and is

composed of a ferritin light chain and FTH1 (ferritin heavy chain). Studies have shown that ferritin and iron levels are increased in osteosarcoma cells, thereby inducing ROS injury. In this study, we used erastin and ferrostatin-1 (an inhibitor of erastin-induced ferroptosis) to verify the effects of curcumin on ferroptosis. Taken together, these results revealed that curcumin could induce cell ferroptosis by regulating the expression of ROS and Nrf2/GPX4 relative protein levels.

Conclusions

In conclusion, our study not only revealed the therapeutic effects of curcumin on osteosarcoma cells and mice models but also revealed the relationship between curcumin and the Nrf2/GPX4 signaling pathway. Our study revealed that curcumin has therapeutic effects on osteosarcoma by regulating the Nrf2/GPX4 signaling pathway.

AUTHORS' CONTRIBUTIONS

All authors participated in the design, interpretation of the studies and analysis of the data, and review of the manuscript. CY, YL, KZ, and RF conducted the experiments. YW gathered and analyzed the subjects' data. RF prepared for the figures. CY and YL wrote the manuscript.

DECLARATION OF CONFLICTING INTERESTS

The author(s) declared no potential conflicts of interest with respect to the research, authorship, and/or publication of this article.

FUNDING

The author(s) disclosed receipt of the following financial support for the research, authorship, and/or publication of this article: This study was supported by the Traditional Chinese Medicine Technology Project of Shandong Province (2020M018).

ORCID ID

Yanchen Liang  <https://orcid.org/0000-0003-0459-5825>

REFERENCES

1. Regan DP, Chow L, Das S, Haines L, Palmer E, Kurihara JN, Coy JW, Mathias A, Thamm DH, Gustafson DL, Dow SW. Losartan blocks osteosarcoma-elicited monocyte recruitment, and combined with the kinase inhibitor toceranib, exerts significant clinical benefit in canine metastatic osteosarcoma. *Clin Cancer Res* 2022;**28**:662–76
2. Shoaib Z, Fan TM, Irudayaraj JMK. Osteosarcoma mechanobiology and therapeutic targets. *Br J Pharmacol* 2022;**179**:201–17
3. Tian H, Cao J, Li B, Nice EC, Mao H, Zhang Y, Huang C. Managing the immune microenvironment of osteosarcoma: the outlook for osteosarcoma treatment. *Bone Res* 2023;**11**:11
4. Shi P, Cheng Z, Zhao K, Chen Y, Zhang A, Gan W, Zhang Y. Active targeting schemes for nano-drug delivery systems in osteosarcoma therapeutics. *J Nanobiotechnology* 2023;**21**:103
5. Ning R, Chen G, Fang R, Zhang Y, Zhao W, Qian F. Diosmetin inhibits cell proliferation and promotes apoptosis through STAT3/c-Myc signaling pathway in human osteosarcoma cells. *Biol Res* 2021;**54**:40
6. Pekarek L, De la Torre-Escuredo B, Fraile-Martinez O, Garcia-Montero C, Saez MA, Cobo-Prieto D, Guijarro LG, Saz JV, De Castro-Martinez P, Torres-Carranza D, Pekarek T, Carrera AC, Alvarez-Mon M, Ortega MA. Towards the search for potential biomarkers in osteosarcoma: state-of-the-art and translational expectations. *Int J Mol Sci* 2022;**23**:14939

7. Zhang W, Wei L, Weng J, Yu F, Qin H, Wang D, Zeng H. Advances in the research of osteosarcoma stem cells and its related genes. *Cell Biol Int* 2022;**46**:336–43
8. Li K, Li D, Zhao L, Chang Y, Zhang Y, Cui Y, Zhang Z. Calcium-mineralized polypeptide nanoparticle for intracellular drug delivery in osteosarcoma chemotherapy. *Bioact Mater* 2020;**5**:721–31
9. Cui J, Dean D, Hornicek FJ, Chen Z, Duan Z. The role of extracellular matrix in osteosarcoma progression and metastasis. *J Exp Clin Cancer Res* 2020;**39**:178
10. Matsuoka K, Bakiri L, Wolff LI, Linder M, Mikels-Vigdal A, Patiño-García A, Lecanda F, Hartmann C, Sibilia M, Wagner EF. Wnt signaling and Loxl2 promote aggressive osteosarcoma. *Cell Res* 2020;**30**:885–901
11. Gao W, Wang X, Zhou Y, Wang X, Yu Y. Autophagy, ferroptosis, pyroptosis, and necroptosis in tumor immunotherapy. *Signal Transduct Target Ther* 2022;**7**:196
12. Li J, Liu J, Xu Y, Wu R, Chen X, Song X, Zeh H, Kang R, Klionsky DJ, Wang X, Tang D. Tumor heterogeneity in autophagy-dependent ferroptosis. *Autophagy* 2021;**17**:3361–74
13. Liu J, Lou C, Zhen C, Wang Y, Shang P, Lv H. Iron plays a role in sulfasalazine-induced ferroptosis with autophagic flux blockage in K7M2 osteosarcoma cells. *Metallomics* 2022;**14**:mfac027
14. Wang Y, Zhang L, Zhao G, Zhang Y, Zhan F, Chen Z, He T, Cao Y, Hao L, Wang Z, Quan Z, Ou Y. Homologous targeting nanoparticles for enhanced PDT against osteosarcoma HOS cells and the related molecular mechanisms. *J Nanobiotechnology* 2022;**20**:83
15. Yan HF, Zou T, Tuo QZ, Xu S, Li H, Belaidi AA, Lei P. Ferroptosis: mechanisms and links with diseases. *Signal Transduct Target Ther* 2021;**6**:49
16. Giordano A, Tommonaro G. Curcumin and cancer. *Nutrients* 2019;**11**:2376
17. Termini D, Den Hartogh DJ, Jaglanian A, Tsiani E. Curcumin against prostate cancer: current evidence. *Biomolecules* 2020;**10**:1536
18. Weng W, Goel A. Curcumin and colorectal cancer: an update and current perspective on this natural medicine. *Semin Cancer Biol* 2022;**80**:73–86
19. Luo H, Lu L, Liu N, Li Q, Yang X, Zhang Z. Curcumin loaded sub-30 nm targeting therapeutic lipid nanoparticles for synergistically blocking nasopharyngeal cancer growth and metastasis. *J Nanobiotechnology* 2021;**19**:224
20. Garufi A, Baldari S, Pettinari R, Gilardini Montani MS, D'Orazi V, Pistritto G, Crispini A, Giorno E, Toietta G, Marchetti F, Cirone M, D'Orazi G. A ruthenium(II)-curcumin compound modulates NRF2 expression balancing the cancer cell death/survival outcome according to p53 status. *J Exp Clin Cancer Res* 2020;**39**:122
21. Vallee A, Lecarpentier Y, Vallee JN. Curcumin: a therapeutic strategy in cancers by inhibiting the canonical WNT/beta-catenin pathway. *J Exp Clin Cancer Res* 2019;**38**:323
22. Sreekanth Reddy O, Subha MCS, Jithendra T, Madhavi C, Chowdoji Rao K. Curcumin encapsulated dual cross linked sodium alginate/montmorillonite polymeric composite beads for controlled drug delivery. *J Pharm Anal* 2021;**11**:191–9
23. Xu C, Wang M, Guo W, Sun W, Liu Y. Curcumin in osteosarcoma therapy: combining with immunotherapy, chemotherapeutics, bone tissue engineering materials and potential synergism with photodynamic therapy. *Front Oncol* 2021;**11**:672490
24. Wang L, Chen X, Du Z, Li G, Chen M, Chen X, Liang G, Chen T. Curcumin suppresses gastric tumor cell growth via ROS-mediated DNA polymerase gamma depletion disrupting cellular bioenergetics. *J Exp Clin Cancer Res* 2017;**36**:47
25. Zuo S, Yu J, Pan H, Lu L. Novel insights on targeting ferroptosis in cancer therapy. *Biomark Res* 2020;**8**:50
26. Cheng T, Zhang Z, Shen H, Jian Z, Li J, Chen Y, Shen Y, Dai X. Topically applied curcumin/gelatin-blended nanofibrous mat inhibits pancreatic adenocarcinoma by increasing ROS production and endoplasmic reticulum stress mediated apoptosis. *J Nanobiotechnology* 2020;**18**:126
27. Sun X, Chen P, Chen X, Yang W, Chen X, Zhou W, Huang D, Cheng Y. KIF4A enhanced cell proliferation and migration via Hippo signaling and predicted a poor prognosis in esophageal squamous cell carcinoma. *Thorac Cancer* 2021;**12**:512–24
28. Wang X, Qin G, Liang X, Wang W, Wang Z, Liao D, Zhong L, Zhang R, Zeng YX, Wu Y, Kang T. Targeting the CK1alpha/CBX4 axis for metastasis in osteosarcoma. *Nat Commun* 2020;**11**:1141
29. Munteanu IG, Apetrei C. Analytical methods used in determining antioxidant activity: a review. *Int J Mol Sci* 2021;**22**:3380
30. Rein ID, Notø HØ, Bostad M, Huse K, Stokke T. Cell cycle analysis and relevance for single-cell gating in mass cytometry. *Cytometry A* 2020;**97**:832–44
31. Qiu Z, Qiu S, Mao W, Lin W, Peng Q, Chang H. LOXL2 reduces 5-FU sensitivity through the Hedgehog/BCL2 signaling pathway in colorectal cancer. *Exp Biol Med* 2023;**248**:457–68
32. Yue A, Chen M, Dai S, Zhang Y, Wei W, Fan L, Wang F, Zhang F, Yu H, Lu Y, Lei Y. Tastin promotes non-small-cell lung cancer progression through the ErbB4, PI3K/AKT, and ERK1/2 pathways. *Exp Biol Med* 2023;**248**:519–31
33. Wang H, Cheng Y, Mao C, Liu S, Xiao D, Huang J, Tao Y. Emerging mechanisms and targeted therapy of ferroptosis in cancer. *Mol Ther* 2021;**29**:2185–208
34. Chen GQ, Benthani FA, Wu J, Liang D, Bian ZX, Jiang X. Artemisinin compounds sensitize cancer cells to ferroptosis by regulating iron homeostasis. *Cell Death Differ* 2020;**27**:242–54
35. Hong-Bin S, Wan-Jun Y, Chen-Hui D, Xiao-Jie Y, Shen-Song L, Peng Z. Identification of an iron metabolism-related lncRNA signature for predicting osteosarcoma survival and immune landscape. *Front Genet* 2022;**13**:816460
36. Chen B, Lee JB, Kang H, Minden MD, Zhang L. Targeting chemotherapy-resistant leukemia by combining DNT cellular therapy with conventional chemotherapy. *J Exp Clin Cancer Res* 2018;**37**:88
37. Stockwell BR. Ferroptosis turns 10: emerging mechanisms, physiological functions, and therapeutic applications. *Cell* 2022;**185**:2401–21
38. Gao M, Yi J, Zhu J, Minikes AM, Monian P, Thompson CB, Jiang X. Role of mitochondria in ferroptosis. *Mol Cell* 2019;**73**:354.e3–63.e3
39. Sun H, Cai H, Xu C, Zhai H, Lux F, Xie Y, Feng L, Du L, Liu Y, Sun X, Wang Q, Song H, He N, Zhang M, Ji K, Wang J, Gu Y, Leduc G, Doussineau T, Wang Y, Liu Q, Tillement O. AGuIX nanoparticles enhance ionizing radiation-induced ferroptosis on tumor cells by targeting the NRF2-GPX4 signaling pathway. *J Nanobiotechnology* 2022;**20**:449
40. Badgley MA, Kremer DM, Maurer HC, DelGiorno KE, Lee HJ, Purohit V, Sagalovskiy IR, Ma A, Kapilian J, Firl CEM, Decker AR, Sastra SA, Palermo CF, Andrade LR, Sajjakulnukit P, Zhang L, Tolstyka ZP, Hirschhorn T, Lamb C, Liu T, Gu W, Seeley ES, Stone E, Georgiou G, Manor U, Iuga A, Wahl GM, Stockwell BR, Lyssiotis CA, Olive KP. Cysteine depletion induces pancreatic tumor ferroptosis in mice. *Science* 2020;**368**:85–9
41. Wei S, Qiu T, Yao X, Wang N, Jiang L, Jia X, Tao Y, Wang Z, Pei P, Zhang J, Zhu Y, Yang G, Liu X, Liu S, Sun X. Arsenic induces pancreatic dysfunction and ferroptosis via mitochondrial ROS-autophagy-lysosomal pathway. *J Hazard Mater* 2020;**384**:121390
42. Liu MY, Li HM, Wang XY, Xia R, Li X, Ma YJ, Wang M, Zhang HS. TIGAR drives colorectal cancer ferroptosis resistance through ROS/AMPK/SCD1 pathway. *Free Radic Biol Med* 2022;**182**:219–31
43. Dinkova-Kostova AT, Copple IM. Advances and challenges in therapeutic targeting of NRF2. *Trends Pharmacol Sci* 2023;**44**:137–49
44. Hayashi M, Kuga A, Suzuki M, Panda H, Kitamura H, Motohashi H, Yamamoto M. Microenvironmental activation of Nrf2 restricts the progression of Nrf2-activated malignant tumors. *Cancer Res* 2020;**80**:3331–44
45. Dodson M, Castro-Portuguez R, Zhang DD. NRF2 plays a critical role in mitigating lipid peroxidation and ferroptosis. *Redox Biol* 2019;**23**:101107